



## Glial-Specific Functions of Microcephaly Protein WDR62 and Interaction with the Mitotic Kinase AURKA Are Essential for *Drosophila* Brain Growth

Nicholas R. Lim,<sup>1,4</sup> Belal Shohayeb,<sup>2,4</sup> Olga Zaytseva,<sup>1,3</sup> Naomi Mitchell,<sup>3</sup> S. Sean Millard,<sup>2</sup> Dominic C.H. Ng,<sup>2,5</sup> and Leonie M. Quinn<sup>1,3,5,\*</sup>

<sup>1</sup>School of Biomedical Sciences, University of Melbourne, Melbourne, VIC 3010, Australia

<sup>2</sup>School of Biomedical Sciences, University of Queensland, St Lucia, QLD 4067, Australia

<sup>3</sup>Department of Cancer Biology and Therapeutics, John Curtin School of Medical Research, Australian National University, Acton, ACT 2601, Australia

<sup>4</sup>Co-first author

<sup>5</sup>Co-senior author

\*Correspondence: [leonie.quinn@anu.edu.au](mailto:leonie.quinn@anu.edu.au)

<http://dx.doi.org/10.1016/j.stemcr.2017.05.015>

### SUMMARY

The second most commonly mutated gene in primary microcephaly (MCPH) patients is *wd40-repeat protein 62* (*wdr62*), but the relative contribution of WDR62 function to the growth of major brain lineages is unknown. Here, we use *Drosophila* models to dissect lineage-specific WDR62 function(s). Interestingly, although neural stem cell (neuroblast)-specific depletion of WDR62 significantly decreased neuroblast number, brain size was unchanged. In contrast, glial lineage-specific WDR62 depletion significantly decreased brain volume. Moreover, loss of function in glia not only decreased the glial population but also non-autonomously caused neuroblast loss. We further demonstrated that WDR62 controls brain growth through lineage-specific interactions with master mitotic signaling kinase, AURKA. Depletion of AURKA in neuroblasts drives brain overgrowth, which was suppressed by WDR62 co-depletion. In contrast, glial-specific depletion of AURKA significantly decreased brain volume, which was further decreased by WDR62 co-depletion. Thus, dissecting relative contributions of MCPH factors to individual neural lineages will be critical for understanding complex diseases such as microcephaly.

### INTRODUCTION

Genome-wide exome sequencing of microcephaly (MCPH) patients identified *wd40-repeat protein 62* (*wdr62*) as the second most commonly mutated gene (Bilguvar et al., 2010; Nicholas et al., 2010; Yu et al., 2010). WDR62 is a ubiquitously expressed cytoplasmic protein in interphase and localizes to the spindle pole in mitosis (Nicholas et al., 2010; Yu et al., 2010). A feature of many WDR62 MCPH-associated alleles is an inability to localize to the mitotic spindle pole (Lim et al., 2015; Nicholas et al., 2010; Yu et al., 2010), and *wdr62* depletion is also associated with defects in spindle and centrosomal integrity, mitotic delay, and reduced brain growth in rodents (Chen et al., 2014; Xu et al., 2014). The neural stem cell (NSC) population gives rise to all neuronal cells in the adult brain. NSC behavior is governed by both cell intrinsic factors and extrinsic factors from the supporting stem cell niche, including the glial lineage, which acts non-autonomously to control stem cell renewal and differentiation of daughters (Cunningham et al., 2013; Florio and Huttner, 2014; Pollen et al., 2015).

The connection between NSCs and their niche, and the importance of spindle integrity to asymmetric division, has been best defined for *Drosophila* NSCs/neuroblasts (NB) (Homem and Knoblich, 2012; Smith et al., 2007; Wirtz-Peitz et al., 2008). WDR62 scaffolds kinases that are important mitotic regulators including c-Jun N-terminal kinase (JNK) members of the mitogen-activated protein kinase superfamily and Aurora kinase A (AURKA) (Chen et al.,

2014; Lim et al., 2015; Xu et al., 2014). In flies, AURKA regulates NB proliferation and is required for the localization of mitotic NB polarity complex protein Bazooka (mammalian Par3) to the apical Par complex (comprising the Par anchor, Inscuteable [Insc] adaptor protein, and Gai/Pins/Mud complex). This establishes the apical-basal NB axis essential for self-renewal and differentiation. As a consequence, mutant *aurka* causes NB overproliferation and tissue overgrowth (Atwood and Prehoda, 2009; Smith et al., 2007; Wirtz-Peitz et al., 2008). The WDR62 ortholog in *Drosophila* (*dWDR62*) is required for brain growth (Nair et al., 2016), but whether signaling between WDR62 and AURKA modulates brain development has not been reported.

In addition to the NB lineage, *Drosophila* studies suggest that the glial lineage governs overall brain volume (Pereanu et al., 2005) through regulation of cell-cycle re-entry and neuroepithelial expansion of NBs (Chell and Brand, 2010; Morante et al., 2013). However, potential contribution(s) of individual brain lineage(s) (NB or glia) to the defective brain growth associated with global depletion of *wdr62* or *aurka* is currently unclear. Here, we confirm that WDR62 is required for spindle orientation in NBs (Nair et al., 2016), however, *wdr62* depletion specifically in NBs does not significantly retard brain growth. Rather, control of brain growth predominantly depends upon glial lineage function, as depletion of either *aurka* or *wdr62* specifically in the glial lineage significantly reduces brain volume. Moreover, although *wdr62* depletion suppressed brain overgrowth associated with *aurka* depletion in NBs, *wdr62*

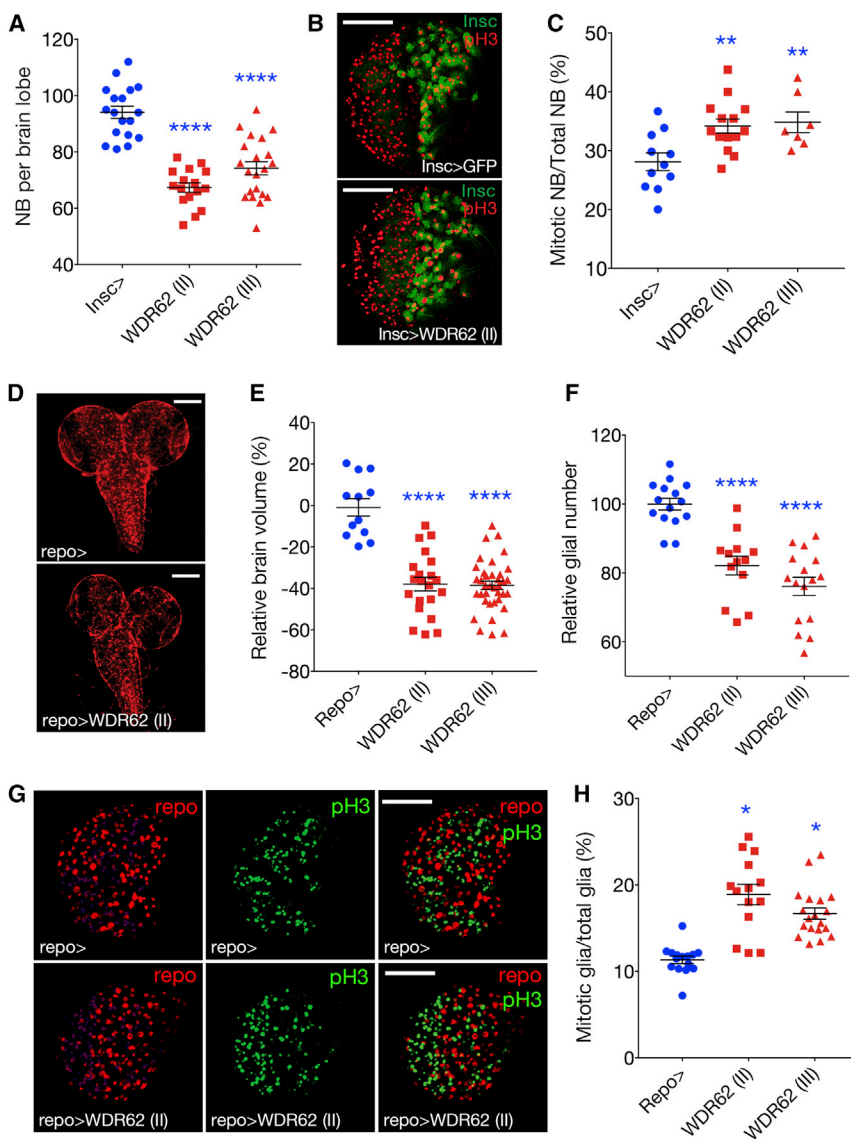


**Figure 1. Glial-Driven Knockdown of WDR62 Decreases Brain Volume**

(A) NBs per third instar larval brain lobe (96 hr after larval hatching [ALH]) for control and *WDR62* RNAi (II) or (III) knockdown (ANOVA,  $p < 0.0001$ ). (B) Mitotic cells in brain lobes marked with anti-phosphohistone H3 (pH3). *Insc*-GAL4 in NBs and INPs marked with GFP. (C) Quantification of mitotic NBs as a percentage of total NB (ANOVA,  $p = 0.0043$ ) (no. of brains: *Insc*-GAL4 = 11, si*WDR62* (II) = 14, si*WDR62* (III) = 7). (D) Control and *WDR62* knockdown *Repo*-GAL4 in glia marked with GFP. (E) Brain lobe volume (ANOVA,  $p = 0.0022$ ). (F) Total glial volume (ANOVA,  $p < 0.0001$ ). (G) anti-pH3 and *Repo*. (H) Mitotic glia as a percentage of total glia (ANOVA,  $p < 0.0001$ ). At least 12 brains were quantified across three independent experiments.

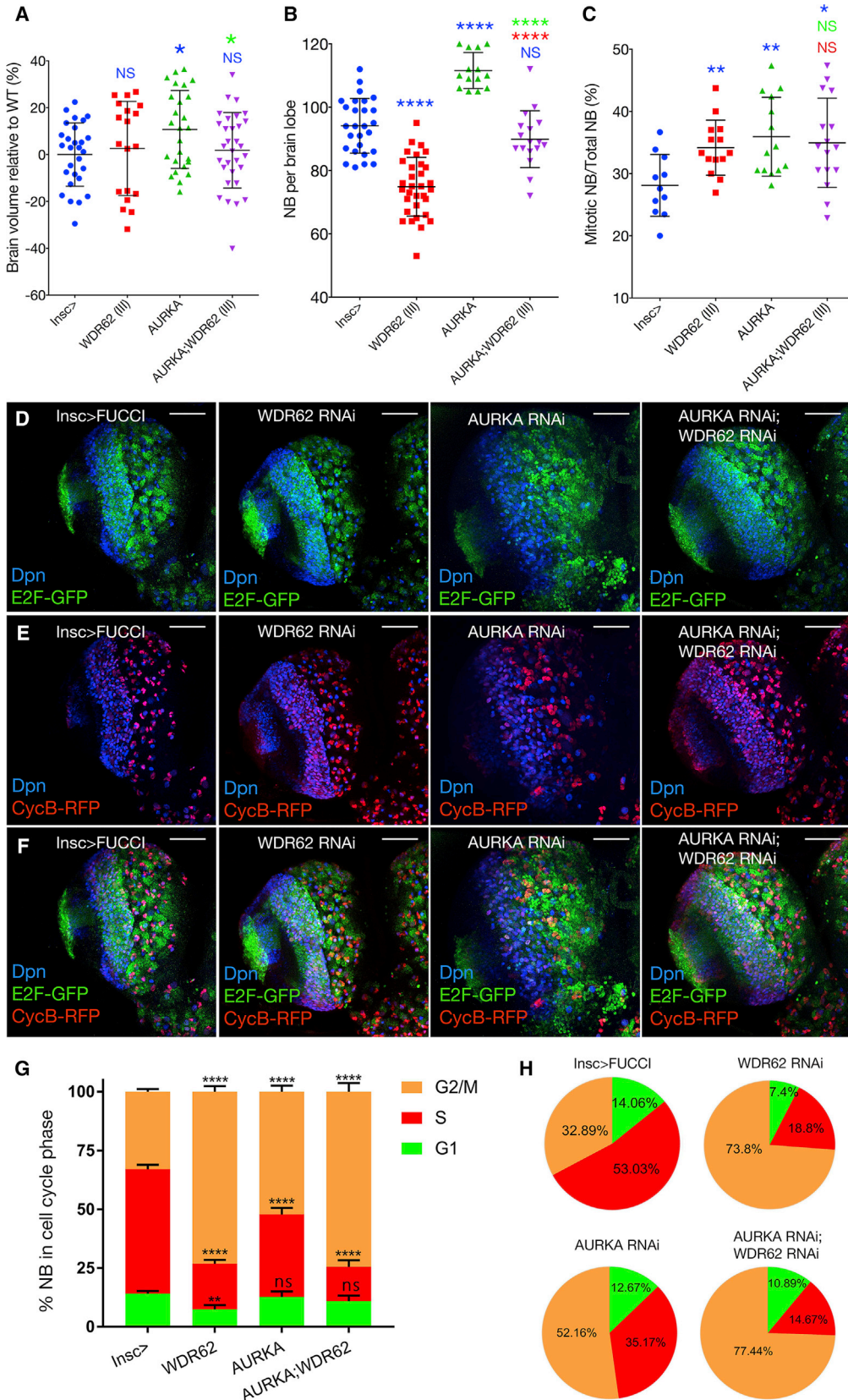
knockdown specifically in the glial lineage enhanced the small brain phenotype associated with *aurka* depletion. Collectively, our data suggest that WDR62 function is negatively regulated by AURKA in NBs but positively regulated by AURKA in glia, and thus demonstrates that lineage-specific signaling functions of AURKA-WDR62 in *Drosophila* orchestrate larval brain growth and development.

## RESULTS

### WDR62 Is Required for Spindle Orientation and Mitotic Progression in NBs

To dissect the contribution of WDR62 to the NB and glial lineage during brain development, we used two alternate

*UAS-wdr62* RNAi lines (to non-overlapping regions of *cg7337*, VDRG #110764 [on chromosome 2], NIG 7337-R1 [on chromosome 3] referred to here as WDR62 [II] and [III]). qPCR revealed a significant decrease in mRNA abundance following ubiquitous *wdr62* knockdown (Figure S1A). In the developing *Drosophila* brain, NBs give rise to intermediate progenitors and ganglion mother cells that differentiate into neurons (Betschinger et al., 2006; Homem and Knoblich, 2012; Knoblich, 2008; Lancaster and Knoblich, 2012). Depletion of *wdr62* in type I and II NB and intermediate progenitors (INP), using *Insc*-GAL4 (Betschinger et al., 2006), decreased NB number (Figure 1A) but did not significantly alter brain volume (Figure S1B). *wdr62* knockdown was not associated with altered timing of major developmental stages (Figure S1C). Thus, analyses



(legend on next page)



conducted on brains of equivalent developmental stages revealed that a significant decrease in NBs does not necessarily manifest in a global reduction in brain growth.

In control third instar larval brains, 28.1% of total NBs are mitotic and *wdr62* depletion significantly increased the mitotic index (Figures 1B and 1C), which suggests a mitotic delay. Decreased NBs are unlikely a consequence of increased cell death, as cleaved caspase-3-positive NBs were unchanged (Figure S1D). The bipolar mitotic spindle must be properly orientated, bisecting the apical and basal crescents of the polarity factors inherited by daughter cells, to ensure timely mitotic progression and asymmetric division of NBs (Knoblich, 2008). *Worniu*-GAL4 driven depletion of *wdr62* caused spindle misorientation (Figure S1E), consistent with previous reports of spindle alignment defects in *wdr62* loss-of-function mutants (Nair et al., 2016). However, further studies are required to determine if this contributes to the increased mitotic index in *wdr62* loss-of-function NBs as spindle misorientation alone is not sufficient to cause cell-cycle delay (Homem and Knoblich, 2012).

How can brain size remain unchanged despite the number of NBs decreasing? One possible explanation could be compensatory proliferation of progeny cells. To determine progenitors in G1, S, or G2M, fluorescence ubiquitination cell-cycle indicator (FUCCI) cell-cycle profiles for deadpan positive G1, S, or G2M cells were subtracted from the total *Insc*-G4 population, which includes NBs and progenitors (Figure S1F). Interestingly, increased S-phase cells were observed in the *Wdr62* knockdown, which suggests that compensatory proliferation of NB daughters might maintain brain size.

### Knockdown of WDR62 in the Glial Lineage Decreases Brain Volume

Depletion of *wdr62* decreased NB number but did not change brain size (Figures 1 and S1F). Pan-glial depletion of *wdr62*, using *Repo*-GAL4 (Sepp et al., 2001), resulted in pupal lethality but did not disrupt larval developmental timing (Figure S1C). *Wdr62* depletion significantly decreased third instar larval brain lobe volume (Figures 1D and 1E), decreased glia (Figure 1F), and increased the mitotic index for remaining glia (Figures 1G and 1H). Thus, *wdr62* loss of function likely results in a mitotic delay in both NBs and glia but is only associated with a signifi-

cant reduction in brain volume when depleted from the glial lineage.

### WDR62 Is Essential for Brain Overgrowth Driven by the Mitotic Kinase AURKA

Previous ex vivo studies suggest AURKA binds WDR62 and regulates its trafficking to the mitotic spindle pole and, thus, spindle integrity (Lim et al., 2015, 2016). To explore potential connections between the AURKA signaling nexus and WDR62 in vivo, we took advantage of the WDR62 brain phenotypes. As qPCR following global *aurka* depletion revealed a relative decrease of 65% for RNAi II and 26% for III, respectively (Figure S1A), RNAi II was used for all subsequent studies. *Insc*-driven depletion of *aurka* significantly increased brain volume (Figure 2A), consistent with brain overgrowth reported for *aurka* mutants (Lee et al., 2006; Wang et al., 2006). Interestingly, brain overgrowth associated with *aurka* depletion in NBs depends on endogenous levels of *wdr62* as co-knockdown brought brain volume back to within the control range (Figure 2A). In line with the increased brain volume, *aurka* knockdown significantly increased NB, and co-depletion of *wdr62* restored NB numbers (Figure 2B).

As observed for *wdr62*, *aurka* knockdown also significantly increased mitotic NBs, however, co-depletion of *wdr62* did not further significantly alter mitotic NBs compared with depletion of *aurka* alone (Figure 2C). To further dissect cell-cycle defects and monitor the timing of gap phases, we used FUCCI to identify G1, G2/M, and S-phase NBs and INP daughters (Zielke et al., 2014). *Insc*-driven FUCCI for individual depletion of *wdr62* or *aurka* revealed increased NBs in G2/M (Figures 2D–2H, control 33%, *wdr62* 74% or *aurka* 52%). Co-depletion resulted in a further significant increase in G2/M NBs compared with individual depletion of *aurka*, but not *wdr62*. These data together with observations that co-depletion did not significantly increase mitotic NBs, compared with individual depletion of *wdr62* or *aurka* (Figure 2C), suggests that *wdr62* depletion extends G2, whether alone or in the *aurka* background.

S-phase NBs (normally 53%) were significantly reduced for both *wdr62* (19%) or *aurka* knockdown alone (35%), and the effect was much more pronounced for *wdr62* RNAi (i.e., compared with *aurka* alone), which brought S phases in the *aurka* RNAi background to within the range of

### Figure 2. WDR62 Is Required for NB Expansion and Brain Overgrowth Associated with Depletion of AURKA

(A–C) Brain lobe volume (A) (ANOVA,  $p = 0.0883$ ), neuroblast number per brain lobe (B) (ANOVA,  $p < 0.0001$ ), mitotic neuroblast as a percentage of total NB (C) (ANOVA,  $p < 0.01$ ) for genotypes marked.  
(D–F) *Insc*-GAL4-driven FUCCI for control or *WDR62* (III) and/or AURKA (II) RNAi. (D) *E2F*-GFP marks G1 cells counterstained with deadpan for NBs, (E) *CycB*-RFP marks S phase, (F) overlap of *CycB* and *E2F* (yellow) marks G2/M.  
(G) Quantification of FUCCI in neuroblasts (ANOVA,  $p < 0.0059$ ).  
(H) Cell-cycle distribution of NBs. At least 11 brains were quantified across three independent experiments.



*wdr62* knockdown alone (15%; **Figures 2G** and **2H**). The reduced proportion of S-phase cells further suggested that *wdr62* depletion reduces NB expansion and prevents brain overgrowth associated with *aurka* knockdown by increasing the G2 delay in NBs. Conversely, the observation that NB loss associated with *wdr62* depletion is reversed by *aurka* co-knockdown is consistent with AURKA behaving as a negative regulator of cell-cycle progression in NBs and WDR62 being required for maintenance of NB proliferation.

### Glial Depletion of AURKA Reduces Brain Size and Enhances the WDR62 Phenotype

As the decreased NB number associated with WDR62 loss of function can be restored by co-depletion of *aurka*, we sought to test if AURKA might modify the glial-dependent decreases in brain size following *wdr62* depletion. In contrast to the increased brain size associated with *aurka* depletion in NBs, *aurka* knockdown in glia significantly decreased larval brain volume (**Figures 3A** and **3B**), as observed for WDR62 (also **Figure 2E**). Moreover, co-depletion of *wdr62* and *aurka* further decreased brain lobe volume and glial number compared with depletion of either *wdr62* or *aurka* alone (**Figures 3A–3C**). Glial cell apoptosis was significantly increased following individual knockdown and further increased following co-depletion compared with *aurka* ( $p = 0.003$ ) but not *wdr62* knockdown in isolation (**Figure S2**).

Glial depletion of *aurka* increased mitosis, and co-depletion with *wdr62* further increased the mitotic index (**Figure 3D**) and the G2/M delay (**Figures 4A–4E**). Although G1 was truncated following *wdr62* or *aurka* depletion alone, the proportion of S-phase glia increased. Interestingly, co-depletion increased the proportion of G1 cells and reduced S phase compared with individual knockdown, suggesting potential roles for the WDR62 and AURKA nexus in interphase (**Figures 4D** and **4E**). In contrast to NBs, where AURKA antagonizes WDR62 function in NB proliferation, our data suggest that AURKA likely cooperates with WDR62 to regulate glial cell number.

In support of the observation that the glial lineage provides a supportive environment for NB renewal and differentiation, *wdr62* depletion in glia significantly decreased NBs (**Figures 3A** and **3E**). Similarly, *aurka* depletion in glia decreased NB number, and co-depletion further significantly reduced NBs compared with individual depletion of *wdr62* or *aurka*. Thus, the associated decrease in brain size may also occur (at least in part) through indirect effects on the NB lineage. To better understand the changes to brain size, we conducted cell-cycle and apoptotic analysis of NBs following manipulation of *wdr62* and/or *aurka* in glia (**Figures 3F–3H**, **Figure S3**). Interestingly, depletion of either *wdr62* or *aurka* in glia significantly increased the

NB mitotic index compared with control ( $p > 0.0001$ ). Although the mitotic index was further significantly decreased following *wdr62* and *aurka* co-depletion in glia compared with *aurka* knockdown alone ( $p = 0.003$ ), it was not significantly different to *wdr62* knockdown in isolation (**Figures 3G** and **S3**). In the same context, a reduction in CycB-positive NBs was observed after knocking down *wdr62* ( $p = 0.0023$ ) or *aurka* ( $p = 0.0363$ ), which was further significantly decreased in the double knockdown compared with *wdr62* ( $p = 0.0019$ ) or *aurka* alone ( $p > 0.0001$ , **Figures 3F** and **S3**).

With regard to apoptosis, following individual knockdown of *wdr62* or *aurka* in glia, we observed a significant increase in apoptotic cell death (marked by cleaved caspase) in NBs compared with control ( $p > 0.0001$ ), although co-knockdown did not further significantly increase NB apoptosis (**Figures 3H** and **S3**). Together these data suggest that the overall decrease in NBs and reduced brain growth, following either *wdr62* or *aurka* knockdown in glia, is due to shortened/accelerated progression through G2 phase and a delay in mitosis, which is accompanied by increased apoptosis that prevents NB expansion.

Using *Wrapper-Gal4* for manipulation of *wdr62* and/or *aurka* in the cortical glial subpopulation, we demonstrated that although individual depletion of *wdr62* or *aurka* did not alter cell death, co-depletion significantly increased apoptosis compared with *wdr62* ( $p = 0.004$ ) or *aurka* alone ( $p = 0.05$ ) (**Figure S4**). Moreover, individual *wdr62* or *aurka* knockdown in the cortical glial subtype did not significantly change proliferation within these glia, NB count, or brain volume, but co-knockdown of *wdr62* and *aurka* significantly decreased both cortical glia ( $p = 0.0177$ ) and NB number ( $p = 0.003$ ) compared with control. This was associated with increased caspase-positive cortical glia ( $p = 0.0074$ ) without a change in brain volume or mitotic cortical glia (**Figure S4**). Although the phenotypes are less severe, these data demonstrate that interaction between WDR62 and AURKA is required autonomously for maintaining the cortical glial subpopulation, and within these cells to support neighboring NB stem cell populations.

## DISCUSSION

In the mammalian brain, radial glia behave as NSCs (**Florio and Huttner, 2014**) that are supported by outer radial glia through cell-cell contact and secretion of growth factors required for maintenance of a stem cell niche (**Pollen et al., 2015**). Another class of glial cells, the microglia population, regulates neural precursor cell numbers to govern final neuronal numbers residing in the cortex (**Cunningham et al., 2013**). However, whether MCPH genes such as

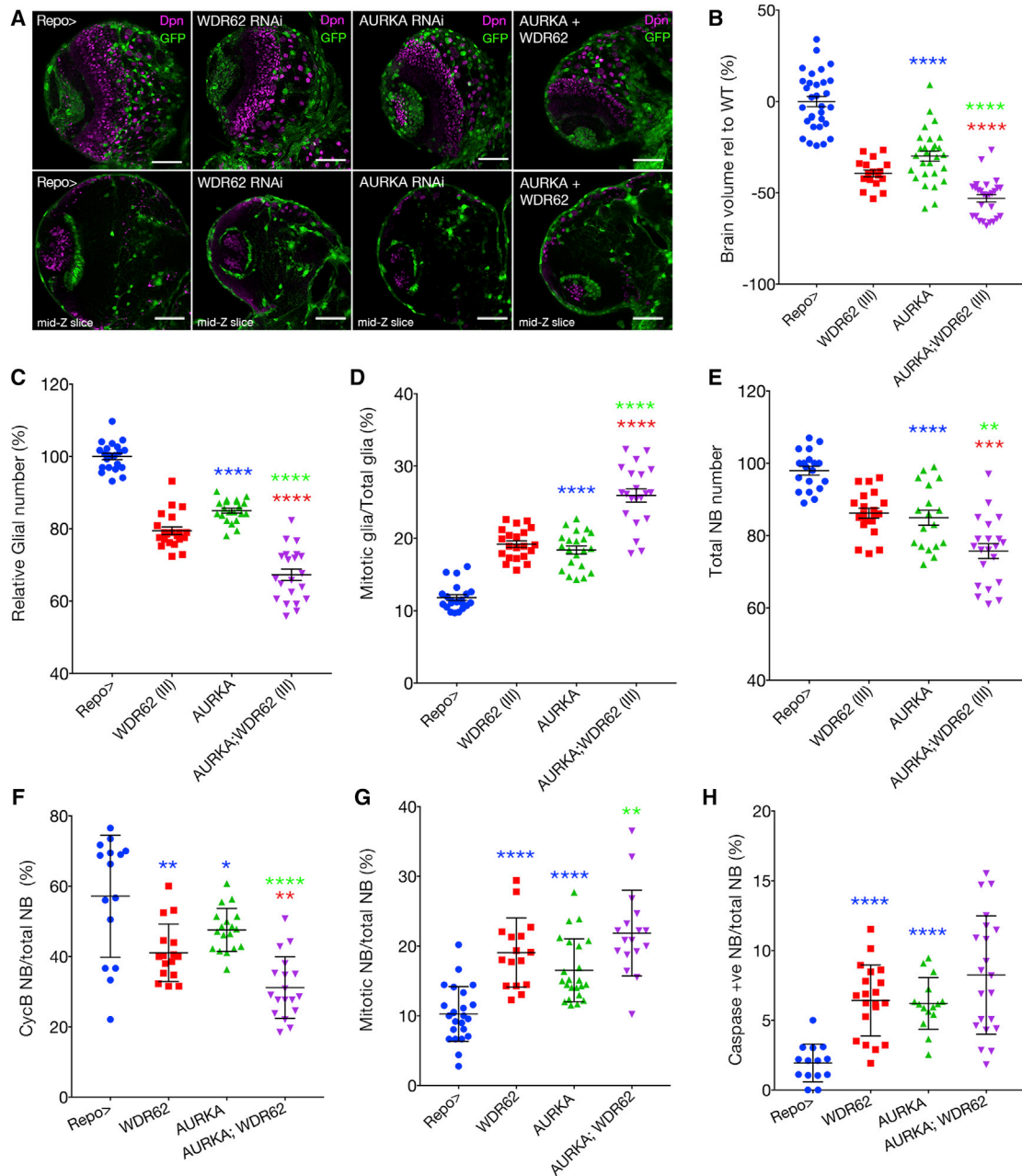


**Figure 3. Glial-Specific Depletion of AURKA Decreases NBs, Glia, and Brain Volume Alone and Enhances the WDR62 Phenotype** (A) *Repo*-driven GFP control, *WDR62* (III) and/or *AURKA* (II) RNAi with Dpn (mid-section of the brain lobe in the lower panel).

(B) Brain lobe volume.

(C–H) Relative glial number (C), neuroblast number (D), mitotic glia (E), CycB-positive neuroblast (F), mitotic neuroblast (G), caspase-positive neuroblast (H). ANOVA,  $p < 0.0001$  for all datasets in this figure. At least 15 brains were quantified across three independent experiments unless stated otherwise.

*wdr62* are important for glial cell fate is unclear. Here, we dissected the lineage-specific contribution of *WDR62* to brain development and revealed that loss of *WDR62* function specifically in the glial, but not the NB lineage, profoundly altered brain growth. Moreover, *wdr62* depletion

in glia likely impairs brain growth autonomously (i.e., through depletion of glia), and also results in NSC loss, suggesting that a focus on *WDR62* function in glia will be integral to elucidating how *wdr62* loss of function contributes to MCPH. That depletion of *wdr62* in the NB



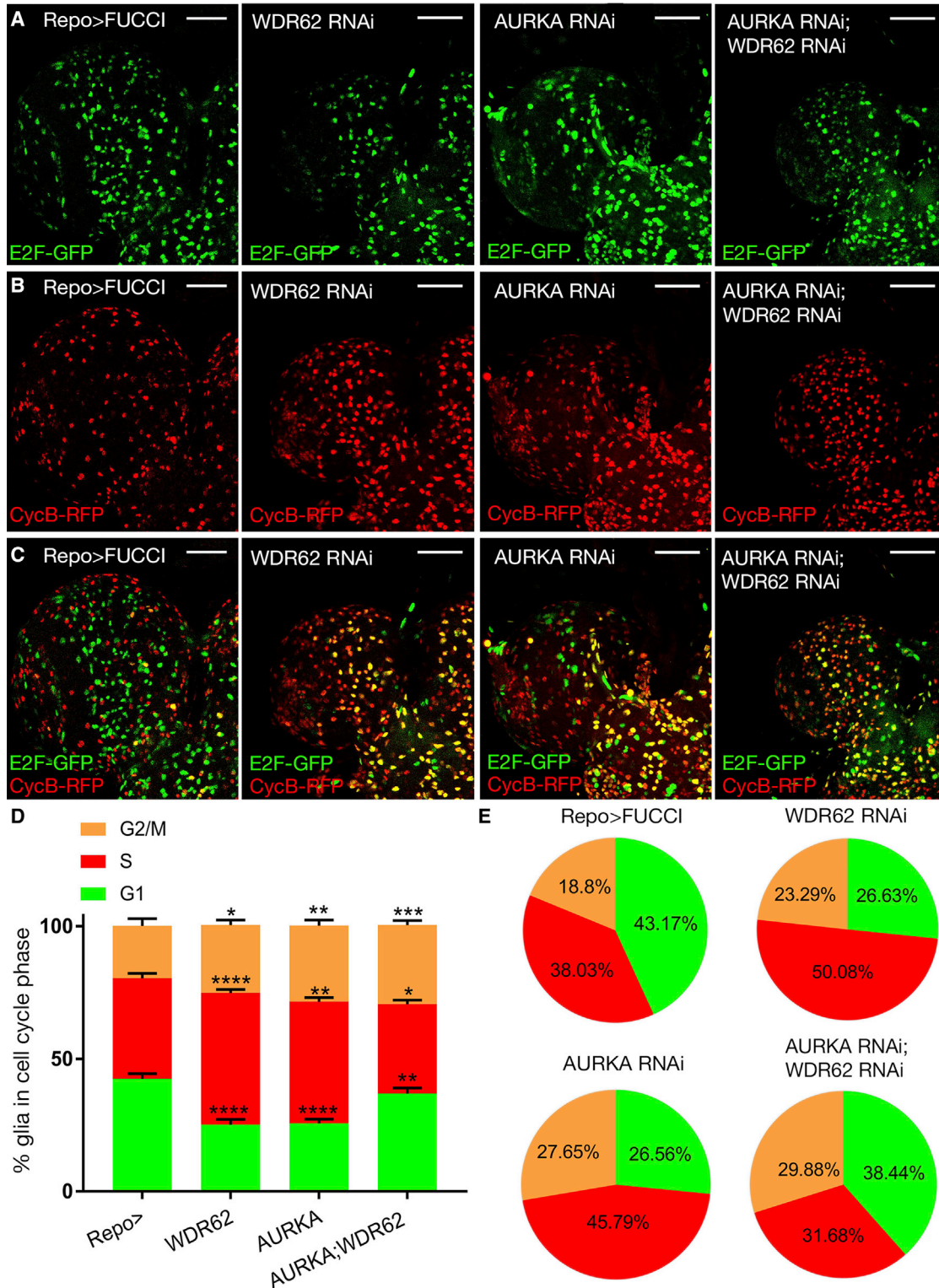


**Figure 4. WDR62 and AURKA Kinase Modulate Cell-Cycle Progression in Glia Cells. Repo-driven *FUCCI* control, *WDR62* (III), and/or *AURKA* (II) RNAi**

(A–C) *E2F-GFP* (A), *CycB-RFP* (B), and overlap (C).

(D) *FUCCI* as a percentage of glial cells. G1 ANOVA,  $p < 0.0001$ ; G2-M ANOVA,  $p < 0.0001$ ; S phase ANOVA,  $p < 0.0091$ .

(legend continued on next page)

lineage was not associated with reduced brain volume, despite reducing NB number, also provides a likely explanation for the recent observation that NB defects associated with global *wdr62* depletion fail to account for reduced brain size (Nair et al., 2016).

Hypomorphic *wdr62* mutant mice have reduced brain size, with associated mitotic defects and an overall decrease in neural progenitor cells (Chen et al., 2014). In *Drosophila*, spindle orientation defects following *wdr62* loss of function likely underlie the G2 delay and increased mitotic figures in NBs (this work and Nair et al., 2016). This phenotype is also reminiscent of the cleavage plane misorientation observed in NSCs in *wdr62*-depleted rat brains (Xu et al., 2014). In *Drosophila* NBs, WDR62 regulates the interphase localization of Centrosomin (CNN, mammalian CDK5RAP2) to the apical centrosome, and thus centrosomal maturation and positioning (Nair et al., 2016). Interestingly, CNN is also an AURKA target that governs spindle orientation independently from cortical polarity establishment during mitosis (Bowman et al., 2006; Lee et al., 2006). Similar to the phenotype observed for *wdr62* depletion in NBs, *cnm* loss of function is associated with spindle orientation defects and reduced NB number (Bowman et al., 2006). Thus, it is tempting to speculate that WDR62 and CNN function in the same AURKA-dependent signaling complex during mitosis.

Ex vivo studies have demonstrated that AURKA phosphorylation of WDR62 promotes spindle pole localization during mitosis (Lim et al., 2015, 2016). Mouse models suggest AURKA and WDR62 interact in vivo to control brain growth (Chen et al., 2014). Compound heterozygous *wdr62<sup>+/-</sup>;aurka<sup>+/-</sup>* mice have a much smaller body size than single heterozygotes but, although the mitotic index of the cerebral cortex was significantly increased and NSCs were reduced, consistent with a mitotic delay radial glia, potential changes to brain volume were not measured (Chen et al., 2014). Here, we demonstrate that the brain overgrowth associated with *aurka* depletion specifically in NBs was suppressed by co-depletion of *wdr62*, bringing brain volume to within the control range. In contrast, the small brain phenotypes, due to glial-specific depletion of either *aurka* or *wdr62*, were further reduced by co-knockdown. Thus, in the context of normal brain development, AURKA likely acts to promote WDR62-dependent glial proliferation, but antagonizes WDR62 function in the NB lineage.

Our findings indicate that WDR62 likely functions in AURKA-mediated regulation of spindle orientation

but not in the establishment of cortical polarity. One reason for the differential output of AURKA regulation of WDR62 (between NB and glia) could stem from the symmetrical nature of glial division, where there is no evidence for cortical polarization. In contrast to the in vivo mammalian studies and previous *Drosophila* studies, which employed global depletion strategies for *wdr62*, our studies have enabled dissection of the relative contribution of *wdr62* loss of function from each of the major brain lineages. In particular, the observation that depletion in either the NB or glial lineage is associated with reduced cell number, but an overall reduction in brain size was only observed when *wdr62* was reduced in glia, places great interest in examining the relative contribution of glial-specific depletion of *wdr62* in mice to brain size. Moreover, future studies of the pathogenic *wdr62* mutations, and identified AURKA phosphorylation sites on WDR62, in the glial lineage are likely to inform on the contribution of this lineage to impaired brain growth in microcephaly.

## EXPERIMENTAL PROCEDURES

### Fly Strains and Crosses

Fly strains were obtained from the following stock collections: Bloomington: *Tub-GAL80<sup>ts</sup>*, *Tub-GAL4*, *Insc-GAL4*, *Wor-GAL4-UAS-Mira-GFP*, *Repo-GAL4*, *UAS-aurka-RNAi (III)* (31704), FUCCI (*UAS-E2F-GFP*, *UAS-CycB-RFP*); VDRC: *UAS-wdr62 RNAi II* (110764), *UAS-aurka-RNAi (II)* (108446); NIG: *UAS-wdr62 RNAi II* (7337-R1). For developmental timing, embryonic lays were conducted at 25°C for 2 hr, prior to a shift to 29°C.

### Immunofluorescence

Developmentally staged late third instar larval heads were fixed in 4% paraformaldehyde/PBS (40 min), washed in PBT (PBS containing 0.1% Tween-20), blocked with 5 mg/mL BSA/PBT, and incubated overnight with appropriate primary antibodies (4°C). After staining with fluorophore-conjugated secondary antibody, samples were counterstained with DAPI and mounted in 80% glycerol for confocal microscopy. 5-Ethynyl-2'-deoxyuridine (EdU) labeling was conducted with the Click-iT EdU Cell Proliferation Assay kit (Life Technologies, cat. no. C10340). Antibodies included mouse anti- $\alpha$ -tubulin (1:200, Sigma DM1A, cat. no. T9026), rabbit anti-cleaved Dcp-1 (1:100, Cell Signaling, cat. no. 9578), rat anti-deadpan (1:100, Abcam, cat. no. ab195173), rabbit anti-pH3 (1:300, Merck, cat. no. 06-570), mouse anti-repo (1:500, DSHB 8D12, cat. no. ab-528448), rabbit anti-pH3 (1:300, Abcam, cat. no. ab47297), rabbit anti-mcherry (1:300, Abcam, cat. no. ab167453), chicken anti-GFP (1:1,000, Invitrogen, cat. no. A10262), and rabbit anti-cycB (DSHB, 1/20).

(E) Cell-cycle distribution of NBs. At least 20 brains were quantified across three independent experiments.

Quantified data represented in all graphs are shown with means and SEM. Statistical tests between two specific datasets are performed with non-paired Student's *t* test with 95% confidence level. Multiple comparison across a given dataset was performed with one-way ANOVA, with Tukey's post-test. Scale bars in all figures represent 100  $\mu$ M (ns,  $p > 0.05$ , \* $p \leq 0.05$ , \*\* $p \leq 0.01$ , \*\*\* $p \leq 0.001$ , \*\*\*\* $p \leq 0.0001$ ).





## Image Acquisition and Data Quantification

Images were acquired on a Zeiss Imager Z confocal microscope with ZEN interface. Analysis of non-deconvoluted images was conducted with Imaris (Bitplane). For brain volume analysis, brain area for each confocal plane was manually demarcated, and volume calculated using compiled area and plane depth. NBs were identified via antibody staining against the NB marker Deadpan, or in the *Insc*-GAL4 background by co-expression of *UAS-GFP*. Similarly, glial cells were identified via staining with anti-repo, or in the *Repo*-GAL4 background by co-expression of *UAS-GFP*. The number of glia or NBs in a confocal stack prepared by an overlapping z series from a third instar brain lobe were quantified automatically using the “spot” function in Imaris quantification software, after applying radius filters according to average cell size. To ensure accuracy of automated data outputs, datasets were selected at random for manual quantification. For co-localization studies (e.g., quantification of mitotic glia) the ImarisColoc function was employed. For Repo FUCCI experiments, glia in G2/M phase were determined by quantifying colocalized E2F-GFP glia and CycB-RFP glia; glia in G1 or S phase were determined by subtracting GFP or RFP glial numbers from the G2/M count, respectively. For *Insc* FUCCI experiments, colocalized GFP and RFP NBs were quantified to determine NBs in G2/M. This number was subtracted from NBs expressing only GFP or RFP to determine G1 or S phase, respectively. In all figures, measurements are represented as a percentage of wild-type measurements.

## qRT-PCR

Late third instar larval heads were dissected and RNA isolated (SV Total RNA Isolation System, Promega), cDNA synthesis performed (Bioline, Tetro cDNA Synthesis Kit) for qPCR (Bioline, SensiFAST SYBR Hi-ROX) performed as described previously (Guo et al., 2016). Briefly reactions were run using Applied Biosystems ViiA7 system in 384-well plates, in technical and biological triplicate. Amplicon specificity was verified by melt curve analysis, average Ct values were calculated for each sample, and fold change was normalized to *Cyp1* and *B-tubulin* housekeeper genes via the  $2^{-\Delta\Delta CT}$  method (Guo et al., 2016). The primers used for the analysis of mRNA levels are as follows:

*cg7337* primer 1 fwd 5'-TGGGGCCTTATCCATACCCA-3'  
rev 5'-GTCATCTGTTGACTGGGCGA-3'  
*cg7337* primer 2 fwd 5'-AAGGATCAGGGCTCGTCTCT-3'  
rev 5'-TGATCTTGATGCACCGCACT-3'  
*aur* primer 1 fwd 5'-AGTATGCGCCACAAGGAA-3'  
rev 5'-CCTGAATATAGGTGGCCGACTGG-3'  
*aur* primer 2 fwd 5'-AGCCCAACAGCGAGAATATGG-3'  
rev 5'-GGAAGCTATGGAATTGGAGCCT-3'

## Statistical Analysis

For an experiment dataset, the data were collected from at least three independent experiments. Statistical significance was calculated with GraphPad Prism 6 using unpaired Student's t test with 95% confidence interval to compare two specific datasets. Multiple comparison across a given dataset was performed with one-way ANOVA, with Tukey's post-test. Scale bars in all figures represent 100  $\mu$ m. In all graphs, the error bars represent SEM. According to

the GraphPad classification of significance points: \* $p < 0.05$ , \*\* $p < 0.01$ , \*\*\* $p < 0.001$ , and \*\*\*\* $p < 0.0001$ .

## SUPPLEMENTAL INFORMATION

Supplemental Information includes four figures and can be found with this article online at <http://dx.doi.org/10.1016/j.stemcr.2017.05.015>.

## AUTHOR CONTRIBUTIONS

N.R.L., B.S., O.Z., and N.M. conceived and conducted experiments and assisted with drafting the manuscript. N.R.L. and B.S. contributed equally as first authors. S.S.M., D.C.H.N., and L.M.Q. conceived experiments and drafted the manuscript. D.C.H.N. and L.M.Q. contributed equally as senior authors.

Received: August 23, 2016

Revised: May 11, 2017

Accepted: May 14, 2017

Published: June 15, 2017

## REFERENCES

- Atwood, S.X., and Prehoda, K.E. (2009). aPKC phosphorylates Miranda to polarize fate determinants during neuroblast asymmetric cell division. *Curr. Biol.* *19*, 723–729.
- Betschinger, J., Mechtler, K., and Knoblich, J.A. (2006). Asymmetric segregation of the tumor suppressor *brat* regulates self-renewal in *Drosophila* neural stem cells. *Cell* *124*, 1241–1253.
- Bilguvar, K., Oztürk, A.K., Louvi, A., Kwan, K.Y., Choi, M., Tatli, B., Yalnizoglu, D., Tüysüz, B., Çağlayan, A.O., Gökben, S., et al. (2010). Whole-exome sequencing identifies recessive WDR62 mutations in severe brain malformations. *Nature* *467*, 207–210.
- Bowman, S.K., Neumüller, R.A., Novatchkova, M., Du, Q., and Knoblich, J.A. (2006). The *Drosophila* NuMA homolog Mud regulates spindle orientation in asymmetric cell division. *Dev. Cell* *10*, 731–742.
- Chell, J.M., and Brand, A.H. (2010). Nutrition-responsive glia control exit of neural stem cells from quiescence. *Cell* *143*, 1161–1173.
- Chen, J.-F., Zhang, Y., Wilde, J., Hansen, K.C., Lai, F., and Niswander, L. (2014). Microcephaly disease gene *Wdr62* regulates mitotic progression of embryonic neural stem cells and brain size. *Nat. Commun.* *5*, 3885.
- Cunningham, C.L., Martínez-Cerdeño, V., and Noctor, S.C. (2013). Microglia regulate the number of neural precursor cells in the developing cerebral cortex. *J. Neurosci.* *33*, 4216–4233.
- Florio, M., and Huttner, W.B. (2014). Neural progenitors, neurogenesis and the evolution of the neocortex. *Development* *141*, 2182–2194.
- Guo, L., Zaysteva, O., Nie, Z., Mitchell, N.C., Amanda Lee, J.E., Ware, T., Parsons, L., Luwor, R., Poortinga, G., Hannan, R.D., et al. (2016). Defining the essential function of FBP/KSRP proteins: *drosophila* Psi interacts with the mediator complex to modulate MYC transcription and tissue growth. *Nucleic Acids Res.* *44*, 7646–7658.



- Homem, C.C.F., and Knoblich, J.A. (2012). *Drosophila* neuroblasts: a model for stem cell biology. *Development* *139*, 4297–4310.
- Knoblich, J.A. (2008). Mechanisms of asymmetric stem cell division. *Cell* *132*, 583–597.
- Lancaster, M.A., and Knoblich, J.A. (2012). Spindle orientation in mammalian cerebral cortical development. *Curr. Opin. Neurobiol.* *22*, 737–746.
- Lee, C.Y., Andersen, R.O., Cabernard, C., Manning, L., Tran, K.D., Lanskey, M.J., Bashirullah, A., and Doe, C.Q. (2006). *Drosophila* Aurora-A kinase inhibits neuroblast self-renewal by regulating aPKC/Numb cortical polarity and spindle orientation. *Genes Dev.* *20*, 3464–3474.
- Lim, N.R., Yeap, Y.Y.C., Zhao, T.T., Yip, Y.Y., Wong, S.C., Xu, D., Ang, C.S., Williamson, N.A., Xu, Z., Bogoyevitch, M.A., and Ng, D.C.H. (2015). Opposing roles for JNK and Aurora A in regulating the association of WDR62 with spindle microtubules. *J. Cell Sci.* *128*, 527–540.
- Lim, N.R., Yeap, Y.Y.C., Ang, C.S., Williamson, N.A., Bogoyevitch, M.A., Quinn, L.M., and Ng, D.C.H. (2016). Aurora A phosphorylation of WD40-repeat protein 62 in mitotic spindle regulation. *Cell Cycle* *15*, 413–424.
- Morante, J., Vallejo, D.M., Desplan, C., and Dominguez, M. (2013). Conserved miR-8/miR-200 defines a glial niche that controls neuroepithelial expansion and neuroblast transition. *Dev. Cell* *27*, 174–187.
- Nair, A.R., Singh, P., Garcia, D.S., Rodriguez-Crespo, D., Egger, B., and Cabernard, C. (2016). The microcephaly-associated protein Wdr62/CG7337 is required to maintain centrosome asymmetry in *Drosophila* neuroblasts. *Cell Rep.* *14*, 1100–1113.
- Nicholas, A.K., Khurshid, M., Désir, J., Carvalho, O.P., Cox, J.J., Thornton, G., Kausar, R., Ansar, M., Ahmad, W., Verloes, A., et al. (2010). WDR62 is associated with the spindle pole and is mutated in human microcephaly. *Nat. Genet.* *42*, 1010–1014.
- Pereanu, W., Shy, D., and Hartenstein, V. (2005). Morphogenesis and proliferation of the larval brain glia in *Drosophila*. *Dev. Biol.* *283*, 191–203.
- Pollen, A.A., Nowakowski, T.J., Chen, J., Retallack, H., Sandoval-Espinosa, C., Nicholas, C.R., Shuga, J., Liu, S.J., Oldham, M.C., Diaz, A., et al. (2015). Molecular identity of human outer radial glia during cortical development. *Cell* *163*, 55–67.
- Sepp, K.J., Schulte, J., and Auld, V.J. (2001). Peripheral glia direct axon guidance across the CNS/PNS transition zone. *Dev. Biol.* *238*, 47–63.
- Smith, C.A., Lau, K.M., Rahmani, Z., Dho, S.E., Brothers, G., She, Y.M., Berry, D.M., Bonneil, E., Thibault, P., Schweisguth, F., et al. (2007). aPKC-mediated phosphorylation regulates asymmetric membrane localization of the cell fate determinant Numb. *EMBO J.* *26*, 468–480.
- Wang, H., Somers, G.W., Bashirullah, A., Heberlein, U., Yu, F., and Chia, W. (2006). Aurora-A acts as a tumor suppressor and regulates self-renewal of *Drosophila* neuroblasts. *Genes Dev.* *20*, 3453–3463.
- Wirtz-Peitz, F., Nishimura, T., and Knoblich, J.A. (2008). Linking cell cycle to asymmetric division: aurora-A phosphorylates the Par complex to regulate Numb localization. *Cell* *135*, 161–173.
- Xu, D., Zhang, F., Wang, Y., Sun, Y., and Xu, Z. (2014). Microcephaly-associated protein WDR62 regulates neurogenesis through JNK1 in the developing neocortex. *Cell Rep.* *6*, 104–116.
- Yu, T.W., Mochida, G.H., Tischfield, D.J., Sgaier, S.K., Flores-Sarnat, L., Sergi, C.M., Topçu, M., McDonald, M.T., Barry, B.J., Felie, J.M., et al. (2010). Mutations in WDR62, encoding a centrosome-associated protein, cause microcephaly with simplified gyri and abnormal cortical architecture. *Nat. Genet.* *42*, 1015–1020.
- Zielke, N., Korzelius, J., van Straaten, M., Bender, K., Schuhknecht, G.F.P., Dutta, D., Xiang, J., and Edgar, B.A. (2014). Fly-FUCCI: a versatile tool for studying cell proliferation in complex tissues. *Cell Rep.* *7*, 588–598.